JOURNAL OF GEOPHYSICAL RESEARCH, VOL. 85, NO. A2, PAGES 664-670, FEBRUARY 1, 1980

Relationship Between Auroral Electrons Fluxes and Field Aligned Electric Potential Difference

M. FRIDMAN

Institut d'Astrophysique, Université de Liège, Liège, Belgium

J. LEMAIRE

Institut d'Aéronomie Spatiale, B-1180 Bruxelles, Belgium

A kinetic theory is used to model the field-aligned distribution of auroral electrons along dipole magnetic field lines. Analytical formulae are obtained for the particle flux ($J_{||}$) and energy flux (ε) as functions of V, the electric potential difference between the equatorial source region and the ionosphere where the accelerated electrons are precipitated and detected by rocket instrumentation. For $1 \ll eV/E_{o||} \ll 500$, ε is nearly proportional to V^2, and $J_{||}$ is proportional to V ($E_{o||}$ is the parallel thermal energy of the electrons; in the plasmasheet, $E_{o||}$ = 0.2–0.6 keV). The observed values for the field-aligned potential drop (V) usually range within the limits defined by this double inequality (i.e., 0.6 kV $\ll V \ll$ 100 kV). The ohmic- like behavior of an auroral magnetic flux tube ($J_{||} \propto V$) and the constancy of ε/V^2 has been found experimentally by Lyons et al. (1979). Using an asymptotic expansion for the kinetic electron precipitation flux and energy flux we have obtained a useful formula which relates the Lyons-Evans-Lundin constant $K(= \varepsilon_{obs}/V_{obs}^2)$ to the auroral electron density and temperature in the source region (i.e., in the plasmasheet).

INTRODUCTION

Using electron observations over several aurorae, *Lyons et al.* [1979] have found that the net downward electron energy flux generally varies as V^2, where V is the field-aligned electric potential difference. The potential difference between the low-altitude point of observation and the high-altitude source region of auroral electrons is inferred from the peak in the observed energy spectra of precipitating electrons. When such a peak is present in the observations, the energy spectra for zero pitch angle electrons can be represented as in Figure 1, taken from *Evans* [1974]. In this model the primary electrons were assumed to have originated from an 800-eV plasma that has been accelerated through a 2-keV potential drop. The lower energy electrons are backscattered secondary electrons produced by the impact of the primary beam of particles, as suggested by *Evans* [1974]. These upgoing secondary electrons are reflected by the potential barrier which accelerated the primary particles downwards.

In absence of collisions, acceleration by a parallel potential V would create a discontinuous spectrum of primary electrons as shown in Figure 1. The source spectra for all downgoing primaries is shifted by an amount $|eV|$ along the energy axis. A bi-Maxwellian distribution for the primary electrons in the source region is assumed,

$$f(\mathbf{v})d\mathbf{v} = N_e\left(\frac{m_e}{2\pi}\right)^{3/2} \frac{1}{E_{o,||}^{1/2}E_{o,\perp}} \cdot \exp\left(-\frac{\frac{1}{2}mv_\perp^2}{E_{o\perp}} - \frac{\frac{1}{2}mv_{||}^2}{E_{o,||}}\right) v_\perp dv_\perp dv_{||} d\varphi \qquad (1)$$

When these electrons are incident upon a parallel potential drop, the differential energy spectra for 0° pitch angles will be given by

$$dJ_{||} \propto E_{||} \exp\left[-(E_{||} - eV)/E_{o,||}\right] dE_{||} \quad \tfrac{1}{2}m_{v||}^2 = E_{||} \geqq eV$$

and

$$dJ_{||} = 0 \quad E_{||} < eV$$

Such an energy spectrum has a local maximum at $E_{||} = E_{0,||}$ if the electrostatic potential drop eV is smaller than the parallel thermal energy $E_{o,||}$ (i.e., when $|eV| < E_{0,||}$). In the other case, when $|eV| > E_{0,||}$, the accelerated primary electrons have a maximum flux at $E_{||} = |eV|$. This is precisely the case illustrated in Figure 1.

Lyons et al [1979] also interpreted the rocket observations made with electrostatic analysers during a series of three flights in the auroral zone, with the assumption that $|eV| > E_{o,||}$. Consequently, the peak in the observed spectra determines the field-aligned potential difference (V) between the ionosphere and the source region, except for small potential differences ($|eV| < E_{0||} \cong$ 200–800 eV). This will be true even if the primary electrons are diffused in energy by wave-particle interactions following their acceleration through the electric potential drop, since such diffusion can smooth the electron distribution but cannot create peaks [*Lyons et al.*, 1979].

The measured slope of the primary electron energy spectra can be used to determine $E_{0||}$, the thermal spread of the source spectrum for 0° pitch angles particles. Similarly, $E_{0\perp}$ can be obtained from the observations when 90° pitch angle flux observations are available. Indeed,

$$dJ_\perp \propto E_\perp \exp\left[-\frac{E_\perp}{E_{0\perp}}\frac{B^s}{B^I} - \frac{E_\perp}{E_{o||}}\left(1 - \frac{B^s}{B^I}\right)\right] dE_\perp$$

Finally, the total energy flux ε (in erg/cm^2/s) carried by the precipitated electrons can also be deduced from the observed energy spectra. The remarkable result that *Lyons et al.* [1979] have obtained is that ε is proportional to V^2. The constant $K(= \varepsilon/V^2)$, which is known as the Lyons-Evans-Lundin or L-E-L constant K, has not the same value for all auroral events but remains generally unchanged during extended periods of observation (several minutes).

Lyons et al. [1979] also found that ε_{obs} is approximately

Paper number 9A1228.
0148-0227/80/009A-1228$01.00

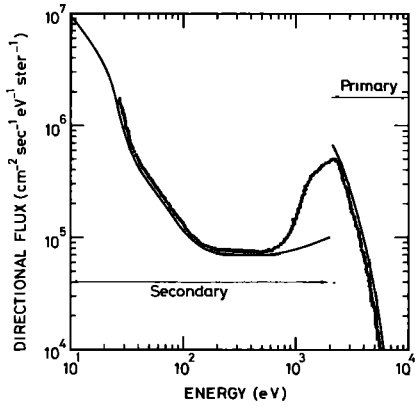

Fig. 1. Auroral electron spectrum. The solid line represents a model calculation by *Evans* [1974] for 0° pitch angle precipitating electrons observed just above the atmosphere. The discontinuity separates electrons of atmospheric origin from those of magnetospheric origin. The primary electrons were assumed to have originated from an 800-eV plasma that had been accelerated through a 2-kV potential drop. The dots illustrate a typical auroral electron spectra, like those often observed. The smoothing of the peak at 2 keV is a consequence of nonadiabatic interaction processes.

equal to $|eV|J_{\|\,obs}$, at least when the lower energy cutoff of electron detectors was high enough to observe only the primary electrons and not the secondary electrons with energies below the minimum in the energy spectrum (see Figure 1).

The purpose of this paper is to show that the Lyons-Lundin-Evans empirical relations can be deduced from the kinetic theory and that these experimental results support collisionless models as those developed by *Lemaire and Scherer* [1971, 1973], *Knight* [1973], and generalized by *Whipple* [1977], *Chiu and Schulz* [1978], *Lemaire and Scherer* [1978], and *Scherer* [1979]. It will be shown that the asymptotic expressions for $\varepsilon(V)$ and $J_{\|}(V)$ are nearly proportional to V^2 and V, respectively, when V is within the range of observed values (i.e., V = 2–20 keV). From the kinetic theory briefly described in the next section, we obtain a useful expression for Lyons-Evans-Lundin constant K which depends on the plasma density and temperature in the high-altitude source region.

The Kinetic Model

Although considered for a long time as rather academic, kinetic or collisionless models have proven to be rather useful in many respects [see *Lemaire and Scherer*, 1974]. The original kinetic models neglecting collisional effects or wave-particle interactions are zero-order approximations which should be improved in the future, through the inclusion of collisions as first-order approximations [*Lemaire*, 1973]. Nevertheless, for the primary auroral electrons ($E > 0.2$ keV) the collisionless approximation is rather satisfactory, at least above 200- to 300-km altitude.

As a result of the conservation of adiabatic invariant and of the total energy of a spiraling electron, one has

$$E_{\|}{}^{I} = E_{\|}{}^{S} - E_{\perp}{}^{S}\left(\frac{B^I}{B^S} - 1\right) + eV \tag{2}$$

$$E^I = E^S + eV \tag{3}$$

E^S and E^I are the energies of an electron in the source region S and in the ionosphere I, repsectively, where it is precipitated and observed; B^I and B^S are the magnetic field intensities in the ionosphere and in the plasmasheet, respectively; note that $B^I/B^S \gg 1$; e.g., for $L = 8$, $B^I/B^S \cong 1000$ and for $L = 10$, $B^I/B^S \cong 2000$.

The diagram of Figure 2 shows two regions in the $(E_{\|}{}^S, E_{\perp}{}^S)$ plane [*Fridman*, 1974]. Each point in this diagram corresponds to an electron energy E and pitch angle θ, i.e., to an electron orbit. The hatched area corresponds to all precipitating particles for which

$$E_{\|}{}^S - E_{\perp}{}^S(B^I/B^S - 1) + eV > 0 \tag{4}$$

When this condition is not satisfied, the particle has a mirror point above the ionosphere and will not contribute to the precipitation flux. See *Whipple* [1977] for a comprehensive discussion of the various classes of orbits when a field-aligned potential is present. Assuming the electric potential $V_{(s)}$ along a magnetic field as a monotonic decreasing function of the altitude s and considering that the potential drop is relatively more concentrated to the region of weak B field such that the condition

$$V_{(s)} - V^s \geq \frac{B_{(s)} - B^s}{B^I - B^s}(V^I - V^s) \tag{4'}$$

is satisfied, one can evaluate the first-order moment of the bi-Maxwellian velocity distribution (1) integrated over the hatched area of Figure 2, which is the downward particle flux $J_{\|}$:

$$J_{\|} = \frac{B^I}{B^S} N_e \left(\frac{E_{0\|}}{2\pi m_e}\right)^{1/2}\left[1 - \frac{\exp(-xeV/E_{0\|})}{1+x}\right] \tag{5}$$

The downward energy flux of electrons is obtained as a third-order moment of the same velocity distribution:

$$\varepsilon = \frac{B^I}{B^S} N_e \left(\frac{E_{0\|}}{2\pi m_e}\right)^{1/2} E_{0\|}\left\{1 + \frac{E_{0\perp}}{E_{0\|}} + \frac{eV}{E_{0\|}} - \exp\left(-\frac{xeV}{E_{0\|}}\right)\left[\frac{E_{0\perp}}{E_{0\|}} + \frac{eV}{E_{0\|}}\left(1 + x\frac{E_{0\perp}}{E_{0\|}}\right)\right]\Big/(1+x) + \frac{1 + xE_{0\perp}/E_{0\|}}{(1+x)^2}\right\} \tag{6}$$

where

$$x = \frac{E_{0\|}}{E_{0\perp}}\,\frac{1}{B^I/B^S - 1} \tag{7}$$

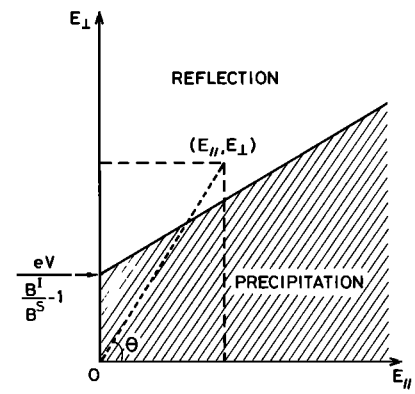

Fig. 2. Phase plane ($E_{\perp}$, $E_{\|}$). Any point in the hatched region determines the energy ($\frac{1}{2} m_e v^2$) and pitch angle θ of an electron which is precipitated into the ionosphere. Particles with larger pitch angle (corresponding to the unshaded region) have a mirror point above the ionosphere.

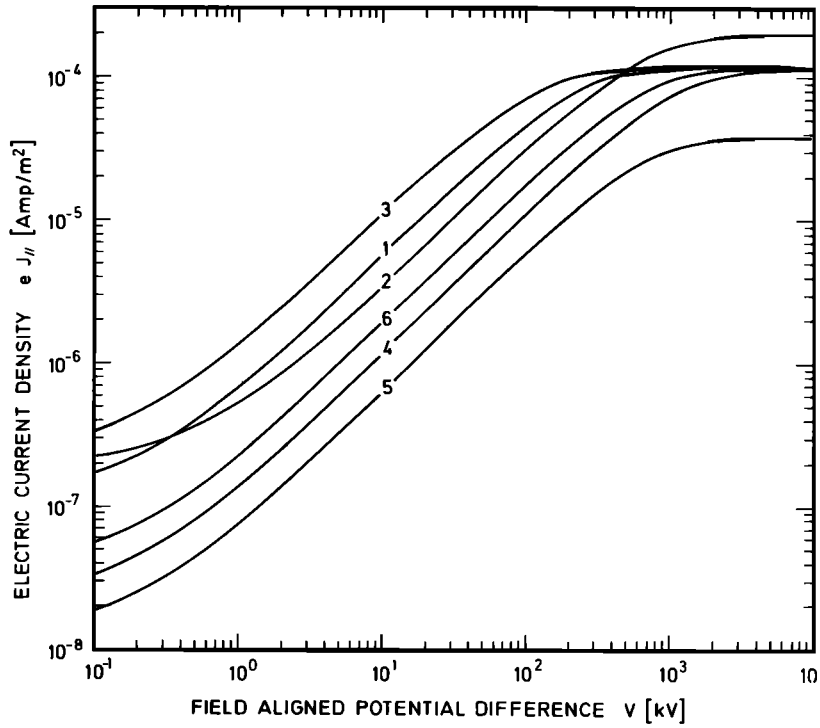

Fig. 3. Characteristic curves showing the field-aligned electric current density (in A/m^2) carried by the hot precipitating electrons as a function of the electric potential difference V (in kV) for six sets of plasma densities and temperatures (given in Table 1) in the source region at $L \cong 8$.

is small compared to unity, unless the velocity distribution is highly anisotropic (i.e., for $E_{0,||}/E_{0,\perp} \gg B^I/B^S \cong 1000$). For $L = 8$–10, $x \cong 0.001$–0.005. $J_{||}$ and ε are nonlinear functions of the field-aligned potential difference V.

Numerical Results

Figure 3 shows the electric current density $eJ_{||}$ (in A/m^2) as a function of V for different values of N_e, $E_{0||}$, $E_{0\perp}$, and B^I/B^S given in Table 1.

It can be seen that the current density carried by the precipitated electrons varies by several orders of magnitude when the potential V varies from 10^{-1} to 10^4 kV. Since the maximum observed field-aligned current measured in auroral events does not in general exceed 10^{-5} A/m^2, one can conclude that the field-aligned electric potential is generally below 100 kV.

This current density is proportional to N_e, the density of hot electrons in the source region, and depends on the thermal spread ($E_{0||}$) and on the pitch angle anisotropy ($E_{0||}/E_{0\perp}$). There is a large range of V values for which the slope of the 'characteristic curves' ($eJ_{||}$, V) is almost independent of V, i.e., where $eJ_{||}$ is a linear function of the applied potential difference V, as in an ohmic conductor. Although collisions are fully neglected in these calculations, there is a domain of V values for which convergent magnetic flux tubes behave as linear or ohmic conductors, whose resistance (or impedance $Z = dV/dJ_{||}e$) is then equal to $E_{0\perp}(2\pi m_e)^{1/2}/(E_{0||}{}^{1/2}e^2N_e)$ (see also below).

For $V < 1\ kV$ and $V > 100\ kV$ the field-aligned system becomes a nonlinear conductor (nonohmic-like conductor). The impedance is always positive for any value of V. For very large values of the applied potential difference, Z tends to infinity and $J_{||}$ tends asymptotically to a maximum value (saturation plateau) which is equal to $(B^I/B^S)N_e(E_{0||}/2\pi m_e)^{1/2}$.

The 'characteristic curves' shown in Figure 3 are similar to the curve given in Figure 1 of the article by *Lemaire and Scherer* [1974]. Note, however, that in the present paper we consider only the partial electric current carried by the hot precipitating electrons, while in the latter reference the authors have considered the total electric current, including the partial currents carried by other electric charges (i.e., the precipitation hot protons, the escaping cold electrons and ions of the ionosphere) which also are present in the physical system. But except for very small field-aligned potential differences (i.e., $V <$ 1–2 eV), the total current density $e(-J_{||}^{\text{hot }e} + J_{||}^{\text{hot}p} - J_{||}^{\text{cold }e} + J_{||}^{\text{cold ions}})$ is almost equal to the current density due to the hot

TABLE 1. Boundary Conditions in the Source Region

Model	1	2	3	4	5	6
N_e, cm^{-3}	0.3	0.3	0.3	0.3	0.1	0.3
$E_{0||}$, keV	0.2	0.6	0.2	0.2	0.2	0.2
$E_{0\perp}$, keV	0.2	0.6	0.1	1.0	0.6	0.6
B^I/B^S	1000	1000	1000	1000	1000	1000
$T_{0||}$, 10^6 °K	2.32	6.95	2.32	2.32	2.32	2.32
$T_{0\perp}$, 10^6 °K	2.32	6.95	1.16	11.6	6.95	6.95
x	1×10^{-3}	1×10^{-3}	2×10^{-3}	2×10^{-4}	3.33×10^{-4}	3.33×10^{-4}
K, erg/cm^2/s/(kV)^2	0.56	0.32	1.14	0.11	0.063	0.19

electron plasma discussed here and illustrated in Figure 3.

Figure 4 shows the ratio $J_{\parallel}/V$ (in $cm^{-2}\ s^{-1}\ kV^{-1}$) as a function of eV/E_0, for the six cases described in Table 1. This is another way to illustrate that there is a range of values of the normalized potential difference ($eV/E_{0\parallel}$) where the hot electron plasma behaves approximately as an ohmic-like conductor. Indeed $10 < eV/E_{0\parallel} < 100$, the curves in Figure 4 are nearly parallel to the V axis (i.e., independent of V).

Figure 5 shows the variation of the energy flux (ϵ in erg/cm^2/s) carried downward into the ionosphere by the hot electrons accelerated through the field-aligned potential difference V. The six curves shown in Figure 4 correspond again to the boundary conditions given in Table 1. It can be seen that the value of ϵ varies by 9 orders of magnitude when the potential V changes from 0.1 kV to 10^4 kV.

As for $J_{\parallel}$, there is a range of V values where log ϵ is a linear function of log V. Within this range (1–100 kV), d log ϵ/d log $V \cong 2$, and ϵ is approximately proportional to V^2. For $V > 100$ kV the energy flux ϵ increases much more slowly with V.

Figure 6 shows the ratio of ϵ/V^2 (in erg/cm^2/s/kV) as a function of the reduced potential difference $eV/E_{0\parallel}$ for the six boundary conditions given in Table 1. For all six cases there exists a range of values of V,

$$10 < eV/E_{0\parallel} < 100 \tag{8}$$

where ϵ/V^2 is indeed nearly constant as was found experimentally by *Lyons et al.* [1979]. In the next section we will determine the value of this constant, which is equal to the L-E-L constant K.

Asymptotic Formulae

When the potential energy eV is much larger than the thermal energy $E_{0,\parallel}$ but smaller than $E_{0\parallel}/x$, where x is the small quantity defined by (7), asymptotic formulae can be given for (5) and (6). To a second order of approximations one obtains

$$J_{\parallel} = N_e\left(\frac{E_{0\parallel}}{2\pi m_e}\right)^{1/2} \frac{B^I/B^S}{B^I/B^S - 1} \frac{eV}{E_{0\perp}}\left[1 + \frac{E_{0,\parallel}}{eV} + \cdots\right] \tag{9}$$

$$\epsilon = N_e\left(\frac{E_{0\parallel}}{2\pi m_e}\right)^{1/2} \frac{B^I/B^S}{B^I/B^S - 1} \frac{(eV)^2}{E_{0\perp}}\left[1 + \frac{2E_{0\parallel}}{eV} + \cdots\right] \tag{10}$$

for

$$1 \ll eV/E_{0\parallel} \ll x^{-1} \tag{11}$$

It can be seen from (9) that to a first approximation $eJ_{\parallel}$ is a linear function of V as in the case of ohmic conductors.

From (10) we see that ϵ varies as V^2 to a first order of approximation and that ϵ/V^2 (i.e., the L-E-L constant K) is then determined by

$$K = N_e \frac{e^2}{(2\pi m_e)^{1/2}} \frac{(E_{0\parallel})^{1/2}}{E_{0\perp}} \tag{12}$$

If N_e is given in cm^{-3}, $E_{0\parallel}$ and $E_{0\perp}$ in keV, the value of K (in erg/cm^2/s/$(kV)^2$) is simply

$$K = 0.846 \frac{N_e(E_{0\parallel})^{1/2}}{E_{0\perp}} \tag{13}$$

The last line in Table 1 gives the calculated values for the six sets of boundary conditions discussed in our paper. The values of K deduced from the experimental observations range between 0.1 and 0.96 erg/cm^2/s/kV^2 or $(1\text{–}9.6) \times 10^{-10}$ A/V-m^2 when correct transformation is made to the MKS unit system. It can be seen that these values are of the same order of magnitude as those given in Table 1 from (13).

The dashed lines in Figure 6 illustrate the asymptotic relation (10) at the first-order approximation. The departures from the actual values are small when $eV/E_{0\parallel}$ satisfies the inequalities (11).

Since x is of the order of 2×10^{-3} or smaller (see Table 1), the range of validity (11) for the asymptotic expansions is

$$1 \ll eV/E_{0\parallel} \ll 500 \tag{14}$$

Considering that the source electrons have a thermal spread ($E_{0\parallel}$) of the order of 0.2–0.6 keV the inequalities (14) become

$$0.6\ \text{kV} \ll V \ll 100\ \text{kV} \tag{15}$$

The maximum in the precipitating auroral electrons spectra is precisely located within these limits where the asymptotic expression are valid and where the Lyons-Lundin-Evans relation ($\epsilon/V^2 = c^{st}$) is appropriate. Outside of this range of field-aligned potential difference, ϵ is not proportional to V^2, and the more correct equation (6) must be used instead of asymptotic equation (10).

As a consequence, the L-E-L relations happen to be so well satisfied for auroral electrons because the potential difference between the ionosphere and the source region, if any, is usually larger than 0.6 kV but smaller than 100 kV.

Lyons et al. [1979] also have found experimentally that

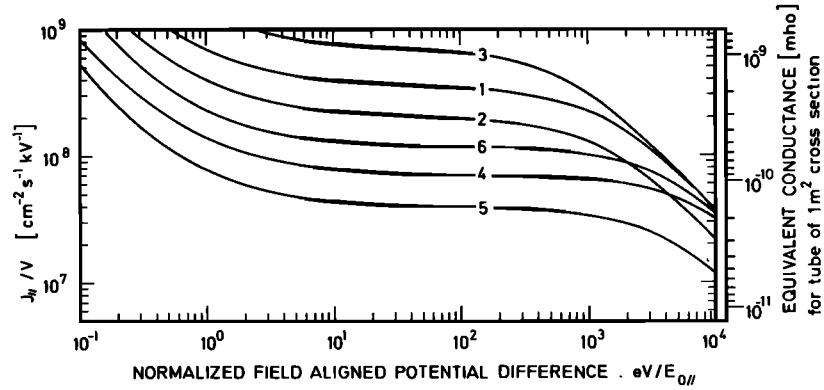

Fig. 4. Ratio of the electron precipitation flux $J_{\parallel}$ (in $cm^{-2}\ s^{-1}$) and field-aligned electric potential V (in kV) as a function of $eV/E_{0\parallel}$, for six sets of plasma densities and temperatures (given in Table 1) in the source region at $L \cong 8$. Note the range of V where $J_{\parallel}$ is proportional to V like in an ohmic conductor. The right-hand scale gives the equivalent load conductance (in mho) for a flux tube of 1-m^2 cross section at the ionospheric level ($\Sigma_{\parallel} \equiv K$).

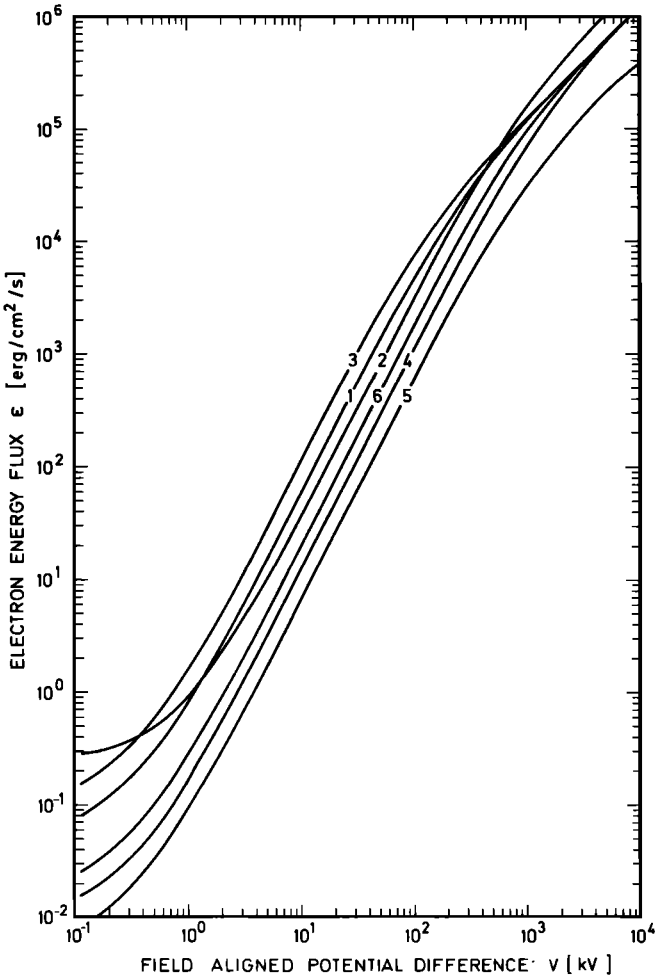

Fig. 5. Downward energy flux ϵ (in erg cm^{-1} s^{-1}) carried by the accelerated electrons, as a function of the electric potential difference V (in kV) for six sets of plasma densities and temperatures (given in Table 1) in the source region at $L \cong 8$.

$$\epsilon_{obs} \cong |eV|\, J_{\|,obs} \tag{16}$$

Figure 7 gives the distribution of $\epsilon/|eV|J_{\|}$ when ϵ and $J_{\|}$ are calculated from (5) and (6). It can be seen that this ratio is nearly the same for all six cases. For $eV/E_{0\|}$ smaller than 1 or 2 the energy flux is significantly larger than $[eV]J_{\|}$, but for larger values of the field-aligned potential difference the experimental relation (16) is also closely satisfied. It is interesting to notice that the range of validity of (16) has no upper limit, unlike the ϵ versus V^2 or the $J_{\|}$ versus V relationships discussed above. Note also that the ratio $\epsilon/|eV|J_{\|}$ is independent of the value of N_e. Therefore even if the value of plasma density (N_e) changes abruptly from one location to the next in the source region, the relation (16) should remain valid, whereas the value of the L-E-L constant K changes in accordance with N_e (see (13)). *Lyons et al.* [1979] have indeed shown a data set indicating that (16) was verified during the whole period of observation, whereas they found it necessary to define two distinct values for K for this same set of observations: i.e., $K = 0.47$ erg/cm^2 s kV^2 corresponding to the 230 first seconds of time, and $K = 0.1$ erg/cm^2 s kV^2 gives a good fit for the observations made during the later portion of the trajectory of the rocket across the auroral form [see Figures 1 and 4 by *Lyons et al.*, 1979]. The experimental results can be interpreted as evidence for a discontinuous change of N_e from one place in the source region to the next. This spatial variation in the plasma density, N_e, produces a comparable variation for ϵ/V^2, but it does not affect the value of the ratio $\epsilon/|eV|J_{\|}$.

Figure 8 is similar to Figure 6. Curve 1 in both figures corresponds to $B^I/B^s = 1000$. For this case as well as for all others considered above, the source region is far away from the ionosphere, i.e., in the low magnetic field region where $B^s \ll B^I$. But the front of the auroral electrons reservoir can extend down the magnetic field lines to rather low altitudes. In this eventuality the ratio B^I/B^s will assume much smaller values. The four other curves in Figure 8 correspond to $B^I/B^s = 500$, 100, 50, and 10, i.e., to a source located respectively at radial distances of 7.4 R_E, 4.3 R_E, 3.5 R_E, and 2.1 R_E along the $L = 8$ magnetic field line. It can be seen that the range of V values, where $\epsilon(V)$ is nearly proportional to V^2, shrinks rapidly when B^I/B^s (or x^{-1}) decrease to values smaller than 100. Therefore it is expected that Lyons-Evans-Lundin's empirical relationships break down when the source of the auroral electrons expands down the magnetic field lines toward lower altitudes.

Discussion and Conclusions

The equations (5) and (6) for the precipitation flux ($J_{\|}$) and energy flux (ϵ) of auroral electrons accelerated through a field-aligned potential difference (V) have been obtained from a simple kinetic theory. The velocity distribution in the source region is assumed to be given by (1). However, the actual velocity distribution of auroral electrons may not necessarily be a bi-Maxwellian. But the results described in the previous paragraph are not critically dependent on the choice of a special function of $f(\mathbf{v})$. When the chosen function has the same first-order moments (N, $\mathbf{J}$, $P_{\perp}$, $P_{\|}$, ϵ, $\cdots$) as the actual velocity distribution at the source one can expect that the calculated distribution of these same moments are very similar to those observed at other altitudes along the magnetic field line [*Lemaire*, 1972].

Furthermore, it appears that the particle populations observed at auroral latitudes [*Croley et al.*, 1978] are separated in the ($E_{\|}$, $E_{\perp}$) plane by recognizable demarcation lines determined from the conservation laws in accordance with Liouville's theorem and in accordance with the kinetic theory used in this and other articles.

It has been shown here that asymptotic formulae (equations

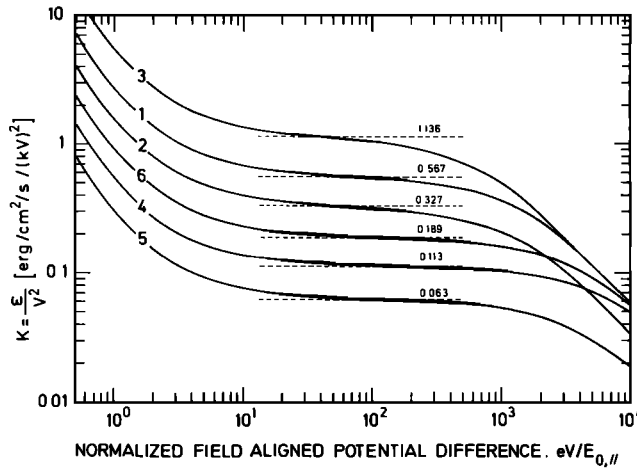

Fig. 6. Ratio of the energy flux ϵ (in erg cm^{-2} s^{-1}) and of V^2 the field-aligned electric potential difference (in kV), as a function of $eV/E_{0\|}$, for six sets of plasma densities and temperatures (given in Table 1) in the source region at $L \cong 8$. Note the range of V where ϵ/V^2 is almost equal to the Lyons-Evans-Lundin constant K.

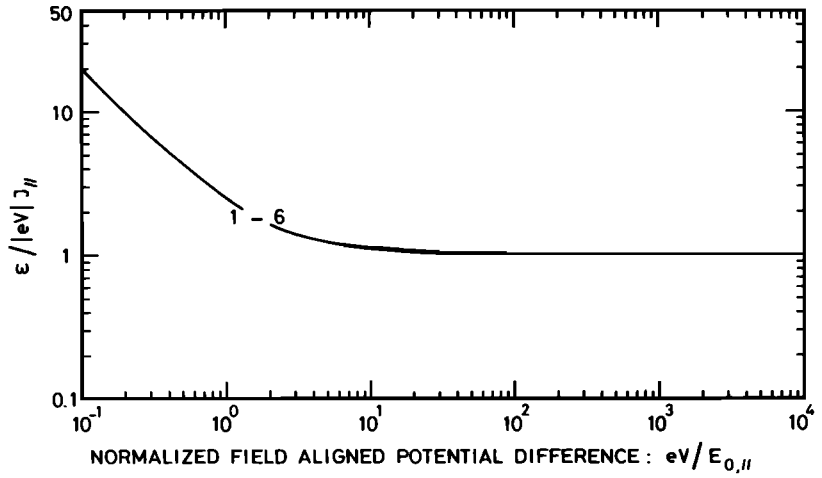

Fig. 7. Ratio of the energy flux ϵ (in erg cm^{-2} s^{-1}) and $|eV|J_{\|}$ (in erg cm^{-2} s^{-1}) as a function of $eV/E_{0,\|}$, for the six sets of plasma densities and temperatures (given in Table 1) in the source region at $L \cong 8$. Note the range of V where ϵ is proportional to $|eV|J_{\|}$ as found experimentally by *Lyons et al.* [1979].

(9)–(10)) can be determined for 0.6 kV $\ll V \ll$ 100 kV. Within this range of values for the field-aligned potential, the energy flux is proportional to V^2, and the electronic current density is a linear function of V like for an ohmic conductor.

The actual field-aligned potential differences, deduced from peaks in the auroral electron spectra, if any, fall within the range of validity of these asymptotic expressions for ϵ and $J_{\|}$. Outside that V range the formulae (5) and (6) must be used instead of (9) and (10).

Lyons et al. [1979] have found experimentally that ϵ/V^2 has a constant value K which, however, may differ from one aurora to another. The experimental values obtained for this L-E-L constant K range within 0.1–1.0 erg/cm^2 s kV^2.

From the kinetic theory we have obtained (12) and (13) which enables us, from experimental measurements of $E_{0\perp}$, $E_{0\|}$ and K (for ϵ/V^2), to infer some approximate value for N_e, the hot electron density in the source region. The value of N_e which can be deduced by this indirect method should be considered as some upper limit value. Indeed, it was assumed that all observed electrons with energies greater than $|eV|$ are 'primaries.' However, since some fraction of backscattered 'primaries' may have energies larger than $|eV|$ [*Evans*, 1974; *Banks et al.*, 1974], the flux of precipitated primary electrons and their energy flux might be smaller than the measured ones. Consequently, the value of N_e deduced from the experimental L-E-L constant K should indeed be considered as some upper limit value. Nevertheless, from low-altitude auroral electron energy spectra and from (13) a maximum value for the electron density in the plasmasheet can be inferred, along the magnetic field line connecting to the point of observation.

The impedance Z of a magnetic flux tube is a function of the hot electron plasma density, temperature, and pitch angle distribution. The load closing the electrical circuit must have an equivalent resistance equal to $V/eJ_{\|}A$ (A is the cross section of the current carrying flux tube). This equivalent conductance is given on the right-hand scale of Figure 4 for a flux tube of one square meter cross section at ionospheric altitude ($\Sigma_{\|} = Z^{-1} = K$).

The assumed field-aligned potential difference (V) can be spread over the whole length of the magnetic field line as in the kinetic models of *Chiu and Schulz* [1978] or *Chiu and*

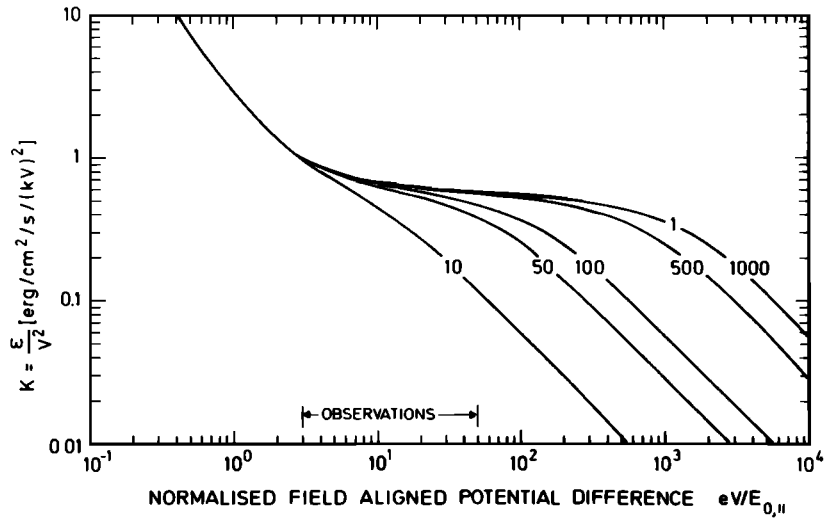

Fig. 8. Ratio of the energy flux ϵ (in ergs cm^{-2} s^{-1}) and of V^2 the field-aligned electric potential difference (in kV), as a function of $eV/E_{0\|}$, for five different values of B^I/B^s ranging between 1000 and 10. Note that when B^I/B^s decreases (i.e., when the altitude of the source of auroral electrons decreases) the range of V where ϵ/V^2 is almost constant becomes narrower.

Cornwall [1980] or over more limited distances. For instance, in the electrostatic shock models of *Kan* [1975], *Swift* [1975, 1976], *Torbert and Mozer* [1978] the average ion gyroradius is the characteristic thickness of the potential layer; in the double layer models of *Block* [1972] and *Lemaire and Scherer* [1978] the Debye length determines the characteristic thickness of the potential layer. Other various spatial distributions of the potential have also been discussed by *Persson* [1966], *Lennartson* [1976, 1977], and *Whipple* [1977]. A review of problems related to macroscopic electric fields in the magnetosphere has been given by *Fälthammar* [1977].

It should be noted that for a given potential difference V between the 'end points' of a magnetic field line, there is not a unique distribution of electric potential (and parallel electric field) between the end points. For given boundary conditions (i.e., the densities, temperatures, pitch angle distributions of the hot and cold ions and electrons) at both ends of a field line, the field-aligned potential distribution is not necessarily a monotonically decreasing function of altitude as is generally assumed in classical stationary kinetic models. Furthermore, there is no clear reason to consider that field-aligned potential distributions can be considered as quasi-stationary as it is usually assumed for convenience. Although the detailed field-aligned structure and time variations of the electric potential are essential to determine the field-aligned density or temperature distributions of the different particles, when condition (4') is verified, such a detailed description is not required to calculate the particles flux and energy flux. Indeed, for a wide range of conditions these quantities are uniquely determined by the total potential difference set up between the source and the sink of accelerated electrons. But an arbitrary amount of trapped particles can change the electron and ion density and therefore change the electric field distribution along the magnetic field lines in almost an unconditional manner.

Acknowledgments. The authors wish to thank E. C. Whipple and L. R. Lyons for stimulating discussions. We also appreciated the constructive suggestions of the referees.

The Editor thanks Y. T. Chiu and W. Lennartsson for their acceptance in evaluating this paper.

REFERENCES

Banks, P. M., C. R. Chappell, and A. F. Nagy, A new model for the interaction of auroral electrons with the atmosphere: Spectral degradation, backscatter, optical emission, and ionization, *J. Geophys. Res., 79,* 1459–1470, 1974.

Block, L. P., Potential double layers in the ionosphere, *Cosmic Electrodynamics, 3,* 349–376, 1972.

Chiu, Y. T., and J. M. Cornwall, Electrostatic model of a quiet auroral arc, *J. Geophys. Res., 85,* this issue, 1980.

Chiu, Y. T., and M. Schulz, Self-consistent particle and parallel electrostatic field distributions in the magnetospheric-ionospheric auroral region, *J. Geophys. Res., 83,* 629–642, 1978.

Croley, D. R., Jr., P. F. Mizera, and J. F. Fennell, Signature of a parallel electric field in ion and electron distributions in velocity space, *J. Geophys. Res., 83,* 2710–2705, 1978.

Evans, D. S., Precipitating electron fluxes formed by a magnetic field aligned potential difference, *J. Geophys. Res., 79,* 2853–2858, 1974.

Fälthammar, C.-G., Problems related to macroscopic electric fields in the magnetosphere, *Rev. Geophys. Space Phys., 15,* 457–466, 1977.

Fridman, M., Flux stationnaires supersoniques de protons paralléles au champ magnétique, *Can. J. Phys., 52,* 2402–2421, 1974.

Kan, J. R., Energization of auroral electrons by electrostatic shock waves, *J. Geophys. Res., 80,* 2089–2095, 1975.

Knight, S., Parallel electric fields, *Planet. Space Sci., 21,* 741–750, 1973.

Lemaire, J., 0^+, H^+, and He^+ ion distributions in a new polar wind model, *J. Atmos. Terr. Phys., 34,* 1647, 1972.

Lemaire, J., Kinetic versus hydrodynamic solar wind models, in *Pleins feux sur la physique solaire,* Centre National de la Recherche Scientifique, Paris, 1978.

Lemaire, J., and M. Scherer, Simple model for an ion-exosphere in an open magnetic field, *Phys. Fluids, 14,* 1683–1694, 1971.

Lemaire, J., and M. Scherer, Plasma sheet particle precipitation: A kinetic model, *Planet. Space Sci., 21,* 281–289, 1973.

Lemaire, J., and M. Scherer, Exospheric models of the topside ionosphere, *Space Sci. Rev., 15,* 591–640, 1974.

Lemaire, J., and M. Scherer, Field aligned distribution of plasma mantle and ionospheric plasmas, *J. Atmos. Terr. Phys., 40* 337–342, 1978.

Lennartsson, W., On the magnetic mirroring as the basic cause of parallel electric fields, *J. Geophys. Res., 81,* 5583–5586, 1976.

Lennartsson, W., On high-latitude connection field inhomogeneities, parallel electric fields and inverted-V precipitation events, *Planet. Space Sci., 25,* 89–101, 1977.

Lyons, L. R., D. S. Evans, and R. Lundin, An observed relation between magnetic field aligned electric fields and downward electron energy fluxes in the vicinity of the auroral forms, *J. Geophys. Res., 84,* 457–461, 1979.

Persson, H., Electric field parallel to the magnetic field in a low-density plasma, *Phys. Fluids, 9,* 1090–1098, 1966.

Scherer, M., Open ion-exosphere with an asymmetric anisotropic velocity distribution, *Aeron. Acta A, 204,* 1979.

Swift, D. W., On the formation of auroral arcs and acceleration of auroral electrons, *J. Geophys. Res., 80,* 2096–2108, 1975.

Swift, D. W., An equipotential model for auroral arcs, 2, Numerical solutions, *J. Geophys. Res., 81,* 3935–3943, 1976.

Torbert, R. B. and Mozer, F. S., Electrostatic shocks as a source of discrete auroral arcs, *Geophys. Res. Lett., 5,* 135–138, 1978.

Whipple, E. C., Jr., The signature of parallel electric fields in the collisionless plasma, *J. Geophys. Res., 82,* 1525–1531, 1977.

(Received April 17, 1979;
revised July 18, 1979;
accepted August 24, 1979.)